Numerical Modeling of Heat-Pipe Transients

W. Jerry Bowman*
U.S. Air Force Academy, Colorado Springs, Colorado 80840

This paper describes work done to increase the understanding of numerical modeling of heat-pipe transients. The most significant contribution discussed in the paper is a method of reducing the amount of computer time required to obtain a numerical solution. It was found that time-accurate results could be obtained even if the heat-pipe's wall model and the heat-pipe's vapor model use different time steps to march through time. This leads to a reduction in computer time requirements by as much as a factor of 500. A second method of decreasing computer time requirements is also discussed. The method involves using an implicit solution algorithm instead of the explicit method used for most of this work. The implicit method was at least 10 times faster than the explicit method. Also in the paper, two different methods for modeling the heat-pipe wall transient are discussed and compared. Both methods gave comparable results; however, one method required less computer time than the other.

Nomenclature

c	=	speed of sound
c_v	=	constant volume heat capacity
E	=	specific total energy
e	=	specific internal energy
f	=	friction coefficient
h_e	=	convection heat transfer coefficient
h_{fg}	=	latent heat vaporization
h_i	=	evaporation/condensation coefficient
k	=	thermal conductivity
p	=	pressure
q''	=	energy flux
R	=	vapor space radius
$\boldsymbol{R}$	=	ideal gas constant
Re	=	Reynolds Number (based on pipe diameter)
r	=	radial coordinate
T	=	temperature
t	=	time
$\boldsymbol{U}, \boldsymbol{F}, \boldsymbol{H}$	=	vector fluxes in vapor equation formulation
u	=	average vapor velocity
V	=	vapor evaporation/condensation velocity
x	=	axial coordinate
α	=	thermal diffusivity
μ	=	vapor viscosity
ρ	=	vapor density
σ	=	time step safety factor
τ_w	=	shear stress between vapor and wall

Introduction

COMPUTER modeling of physical phenomena is an important complement to experimentation. Computer models have the potential of being less expensive and time consuming relative to experimental work once the computational model is verified with the experimental data. Also, computational models simulate property measurements within the physical domain of interest that are impossible or too costly to obtain with experimental methods.

Heat-pipe modeling involves the modeling of several physical processes (Fig. 1). These processes include the following: energy conduction through an evaporator wall; boiling in the heat-pipe evaporator's wick and movement of the resulting vapor away from the evaporator through the heat-pipe vapor space and into the condenser; and energy conduction through the condenser wall. To model wick-liquid dynamics properly, the process of liquid returning to the evaporator end of the heat pipe from the condenser must be modeled. Along with the problem of properly modeling the physics of a heat pipe is the problem of heat-pipe transients occurring slowly. The slow nature of the transients coupled with small time steps used during numerical solutions dictated by stability and accuracy constraints results in large amounts of computer time being required to model the transients.

Several attempts at modeling heat-pipe transients have been made over the last few years.[1-6] Once confidence has been gained in such models, they can be used to predict heat-pipe behavior and obtain insight into heat-pipe operation. This paper describes how a heat-pipe transient was successfully numerically modeled and compares different ways of modeling the heat-pipe wall. Also, an implicit solution technique is compared with an explicit technique to demonstrate which method requires the least amount of computer time to resolve the heat-pipe transient behavior. Most important, methods of accelerating the explicit solution technique are investigated. Throughout the paper, the results from the numerical models are compared to experimental data.

Numerical Model

Vapor Model

Governing Equations and Boundary Conditions

For the numerical vapor model, the flow was assumed to be one dimensional, compressible, and unsteady. Using these assumptions, the continuity equation is

$$\frac{\partial \rho}{\partial t} + \frac{\partial(\rho u)}{\partial x} + \frac{2\rho_w V}{R} = 0 \qquad (1)$$

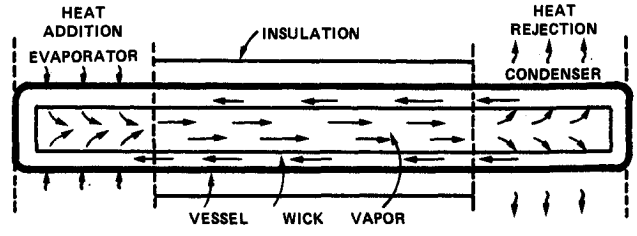

Fig. 1 Basic heat pipe.

Received Nov. 2, 1989; presented as Paper 90-0061 at the AIAA 28th Aerospace Sciences Meeting, Reno, NV, Jan. 8-11, 1990; revision received Aug. 1, 1990; accepted for publication Aug. 15, 1990.

*Assistant Professor, Aeronautical Engineering, HQ USAFA/DFAN. Member AIAA.

The momentum equation is

$$\frac{\partial(\rho u)}{\partial t} + \frac{\partial[\rho u^2 + p - 4/3\mu(\partial u/\partial x)]}{\partial x} + \frac{2\tau_w}{R} = 0 \quad (2)$$

The normal stress term in Eq. (2) was not ignored as is commonly done for a one-dimensional analysis.

The shear stress was modeled as

$$\tau_w = \frac{f\rho u^2}{2} \quad (3)$$

The friction coefficient f will be discussed later in the paper.

Lastly, the energy equation is

$$\frac{\partial(\rho E)}{\partial t} + \frac{\partial[\rho u(E + p/\rho) - k(\partial T/\partial x)]}{\partial x} + \frac{\rho_w V(E + p/\rho)_w}{R} = 0 \quad (4)$$

where $E = e + u^2/2$. The subscript w refers to fluid properties evaluated at the vapor/wick interface condition. Like the normal stress term in Eq. (2), the axial conduction term in Eq. (4) was not ignored. It is has been shown to be very important in the numerical stability of the solution.[6]

The complete set of equations describing the vapor flow can be written in the form

$$\frac{\partial U}{\partial t} + \frac{\partial F}{\partial x} + H = 0 \quad (5)$$

where

$$U = \begin{bmatrix} \rho \\ \rho u \\ \rho E \end{bmatrix} \quad (6)$$

$$F = \begin{bmatrix} \rho u \\ \rho u^2 + p - \frac{4}{3}\mu\left(\frac{\partial u}{\partial x}\right) \\ \rho u(E + p/\rho) - k\left(\frac{\partial T}{\partial x}\right) \end{bmatrix} \quad (7)$$

$$H = \frac{1}{R}\begin{bmatrix} 2\rho_w V \\ 2\tau_w \\ 2\rho_w V(E + p/\rho)_w \end{bmatrix} \quad (8)$$

The boundary conditions used for the vapor space were as follows. At the ends of the vapor space, the axial velocity u was zero and the axial pressure and temperature gradients were zero. Along the length of the heat pipe, the evaporation/condensation mass velocity $\rho_w V$ was specified from the wall model, based on the energy flux leaving or entering the heat-pipe wall using the expression

$$\rho_w V = q''/h_{fg} \quad (9)$$

Vapor Gas Model

The vapor was assumed to be an ideal gas. This meant that the gas' internal energy e was defined as $e = c_v T$. Also, for the ideal gas model, $p = \rho RT$.

Friction Model

For this work, the simplest friction model possible was used to find the friction coefficient f in Eq. (3). In the evaporator and condenser, the vapor flow's Reynolds number was checked to determine if the vapor flow was laminar or turbulent. Local Reynolds numbers (based on pipe diameter) below 2×10^3 indicated laminar flow, and the friction coefficient was given by the equation

$$f = \frac{16}{Re} \quad (10)$$

where $Re = 2\rho uR/\mu$. If the Reynolds number was greater than 2×10^3, the flow was considered turbulent and the friction coefficient was given by

$$f = \frac{0.046}{Re^{1/5}} \quad (11)$$

With the friction coefficient known, shear stress could be found using Eq. (3). A friction model that takes into account mass injection and mass extraction at the vapor/wick interface is available.[7] A preliminary study of this model indicated that it did little to improve the overall heat-pipe numerical model accuracy; however, the more complicated friction model did help the numerical stability of the heat-pipe model.[8]

Wall Model

Governing Equations and Boundary Conditions

For the explicit model, the energy transfer through the wall was assumed to be unsteady and one dimensional at each axial location along the heat pipe; however, each axial location along the heat pipe was studied separately. This allowed for different radial temperature distributions at each axial location. Thus, the temperature in the wall could vary radially, axially, and with time, but no energy conduction was considered axially along the heat-pipe wall. The one-dimensional heat diffusion equation solved at each axial location along the heat pipe during the explicit solution was

$$\frac{1}{r}\frac{\partial}{\partial r}\left(r\frac{\partial T}{\partial r}\right) = \frac{1}{\alpha}\frac{\partial T}{\partial t} \quad (12)$$

For the implicit method, an unsteady, two-dimensional model was used. The two-dimensional heat diffusion equation solved during the implicit solution was

$$\frac{1}{r}\frac{\partial}{\partial r}\left(r\frac{\partial T}{\partial r}\right) + \frac{\partial^2 T}{\partial x^2} = \frac{1}{\alpha}\frac{\partial T}{\partial t} \quad (13)$$

Regarding the wall boundary conditions, on the exterior surface of the evaporator, an energy flux was specified and set equal to the energy conduction at the evaporator's exterior surface

$$q'' = -k\frac{\partial T}{\partial r}\bigg|_{\substack{\text{outside} \\ \text{wall}}} \quad (14)$$

On the inside wall (wall/vapor interface) an evaporation/condensation boundary condition was used. The energy conducted away from (or to) the wall was set equal to the energy absorbed (or given off) by the evaporating (or condensing) fluid.

$$-k\frac{\partial T}{\partial r}\bigg|_{\substack{\text{inside} \\ \text{wall}}} = q'' = h_i(T_{\text{vap}} - T_w) \quad (15)$$

where T_w is the inside wall temperature and T_{vap} is the vapor temperature. Because the vapor temperature was included in this wall boundary condition, the boundary condition coupled the wall and vapor models. Also, the energy fluxes q'' in Eqs. (15) and (9) are the same.

Along the outside of the condenser, the environment temperature was specified and energy conducted out of the wall was set equal to the energy convected to the freestream environment:

$$-k\left.\frac{\partial T}{\partial r}\right|_{\substack{\text{outside}\\ \text{wall}}} = h_e(T_w - T_{\text{env}}) \tag{16}$$

where T_w is the external condenser wall temperature and T_{env} is the environment temperature around the heat pipe.

Wall Thermodynamic Properties

For the simplest explicit model and for the implicit model, the wall, wick, and liquid in the wick were treated as one homogeneous layer. An equivalent thermal conductivity for the wall, thick, and liquid combination was found using an equivalent thermal resistance technique.[9] Mass average properties were used for all other wall properties.

A more complicated explicit model was also studied where the wall was divided into two layers. One layer consisted of the heat-pipe container, the other layer was made up of the wick-liquid combination. Properties for the two layers were different. Properties for the wick/liquid combination were treated as described earlier. The container properties were simply the properties of the container material (copper).

An improvement to the model for future study would be the addition of a dynamic liquid model to study the transient behavior of liquid in the wick.

Evaporation/Condensation Coefficient

The coefficient h_i was assumed to be 2500 W/m^2 K for both evaporation and condensation, which is on the low end of what might be expected for convection with phase change boiling and condensation. This is a good area for model improvement and future study.

Solution Method

Vapor Problem Solution

For the vapor space, two solution techniques were studied. For one model, MacCormack's explicit finite difference method[10] was used to solve Eq. (5). For the implicit model, the Beam and Warming[11] finite difference technique was used.

The stability constraint used for the explicit method was

$$\Delta t = \sigma \Delta t_{\text{CFL}} \tag{17}$$

where Δt_{CFL} is

$$\Delta t_{\text{CFL}} = \left(\frac{u}{\Delta x} + \frac{c}{\Delta x}\right)^{-1} \tag{18}$$

where Δx is the axial grid spacing in the vapor region of the heat pipe.

During the explicit solution process, the time step was recalculated every 10 time steps for each of the axial locations along the vapor space. The smallest of the values found was used to advance the vapor solution 10 more time steps through time.

The implicit solution method had no theoretical stability constraint; however, accuracy requirements placed some limit on the time step that could be used.

Wall Problem Solution

For the wall model, the heat diffusion equation [Eqs. (12) and (13)] were solved using finite difference methods. The stability requirement for the explicit finite differenced heat diffusion equation was

$$\frac{\alpha \Delta t}{(\Delta r)^2} < 1/2 \tag{19}$$

For typical values of thermal diffusivity α, the allowable time step for the wall model was larger than the allowable time step for the vapor model [Eq. (17)]. During the explicit solution, the time step found for the vapor model was used to advance both the wall and vapor solutions through time. Convergence to steady-state results could be accelerated by marching the wall through time using a larger time step than that used for the vapor. For the implicit numerical model, an alternative direction implicit (ADI) solution scheme was used for the wall model.

Time Warping

Time warping is the name used here to describe marching the wall model through time using a different time step than the vapor model. For example, warp 50 means that the wall time step was 50 times larger than the vapor time step. When implemented, the wall model solution was marched one large time step through time and then the vapor model solution was marched one small time step through time. This process is similar to a method called local time stepping. Time warping was attempted in order to decrease the amount of computer time required to model a heat-pipe transient. Best time warping was achieved (most computer time saved) if the vapor and wall models used different time steps, each as close as possible to their respective stability constraints.

The time warping was implemented by first marching the wall model through time one large time step and then marching the vapor model through time one small time step. Thus, the time steps used to perform these two operations were different. Time-accurate solutions were not expected; however, as will be shown later, close to time-accurate solutions were obtained.

Numerical Grid Studies

Whenever using finite differencing techniques to approximate a solution to a differential equation, solution accuracy can depend on grid size. For the explicit model described in this paper, four different grid parameters existed: two spacial grid sizes (axial and radial) and two time step sizes. Two time step sizes were needed because time warping was used. Recall that one time step was used to march the wall solution through time and one was used to march the vapor solution through time.

Figures 2 and 3 summarize the grid studies. For the study, identical heat-pipe transients were studied for different grids and time step sizes. The temperatures presented in Figs. 2 and 3 are the average vapor temperatures after steady state had been reached. In the legend, an $A \times B$ grid corresponds to A grid points in the radial direction and B grid points in the axial direction.

In Fig. 2, the radial grid size was varied. This also resulted in a varing wall model time step size since the two are dependent [Eq. (19)]. In Fig. 2, the time step was nondimensionalized by dividing the actual time step by 80% of the maximum time step associated with three radial grid points. In Fig. 2, it can be seen that radial grid spacing and wall model time step size have little impact on the solution as long as time step size doesn't become small. It can be concluded that using three radial grid points will give as good an answer as using more than three and will also have the benefit of using the least amount of computer time. With the three radial grid points, time steps smaller than 1/64 the maximum allowed will result in some roundoff error, the roundoff error becoming larger with smaller time steps. Time steps larger than 1/64 the maximum gave essentially the same results.

Axial grid spacing and vapor model time step size seem to have a larger impact on solution accuracy than radial grid spacing. Figure 3 illustrates the results of the axial grid study. In Fig. 3, the time step is nondimensionalized with respect to 80% of the maximum time step allowable for 11 axial grid points [Eq. (17)]. Using a vapor time step size of 80% the maximum, as the axial grid was refined from 11 to 21 to 41

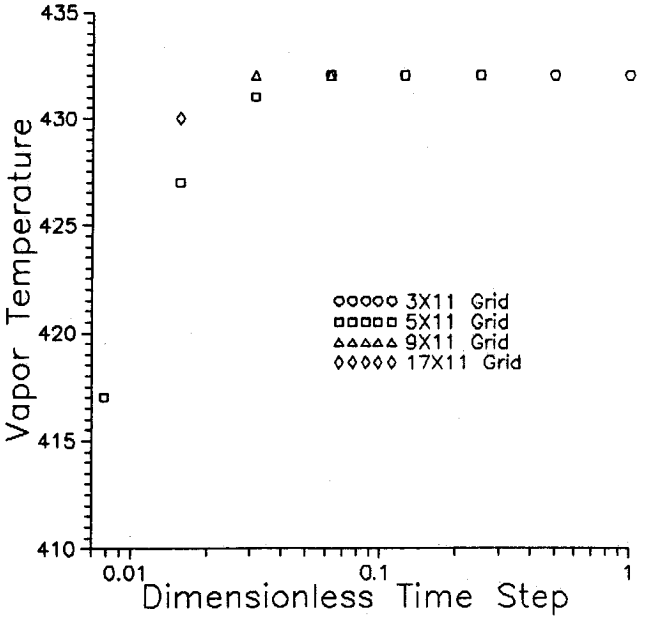

Fig. 2 Results of the radial grid spacing study.

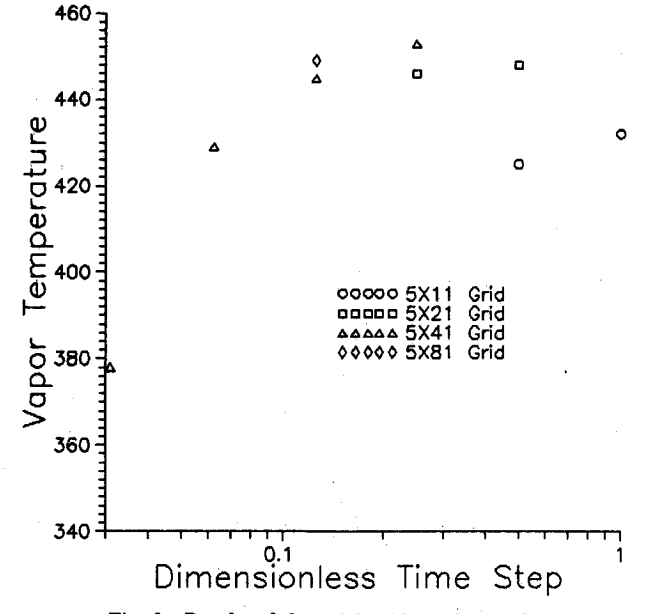

Fig. 3 Results of the axial grid spacing study.

grid points, the final steady-state vapor temperature seemed to converge on slightly over 450 K. When a grid with 81 axial points was used, the solution seemed to begin to diverge, indicating excessive roundoff error. For any one of the axial grids, as the vapor model time step was lowered from 80% the maximum, the final steady-state vapor temperature was lowered. It was concluded that an axial grid of 41 points with as large of vapor model time step as stability constraints would allow would give the most accurate results.

Experimental

A numerical model is not worth much unless it gives accurate results. A standard of comparison is experimental data. As an accuracy check, the numerical results from the models described earlier were compared to experimental data taken by N. Huber and W. Miller in a laboratory class at the U.S. Air Force Academy.

The heat pipe used during the experiment was furnished by the Power Technology Group, Air Force Aero-Propulsions Laboratory of the Air Force Wright Aeronautical Laboratories, Wright-Patterson Air Force Base, Dayton, Ohio. It was 0.61 m long (24 in.) and had an outside diameter of 1.5875 cm (0.625 in.) and a wall thickness of 0.159 cm (1/16 in.). The heat-pipe container and wick were copper and it was filled with 143 cc of water. The wick consisted of four wraps of a 100-mesh/in. copper screen. The total wick thickness was 0.1–0.13 cm. The internal dimensions of the heat pipe were estimations based on standard material dimensions.

The evaporator section of the heat pipe was 0.30 m long. It was wrapped with an electric heating element and then insulated to insure that most of the energy produced by the heater entered the heat pipe. The remainder of the heat pipe was left uninsulated to form the condenser. There was no adiabatic section. The condenser was cooled by free convection to the air around the heat pipe.

The heat pipe was mounted in a horizontal position. Twelve T-type thermocouples were attached to the heat pipe at intervals of 5.08 cm (2 in.). The thermocouple closest to the evaporator end of the heat pipe was 0.64 cm from the end of the heat pipe. The thermocouple closest to the condenser end of the heat pipe was 4.45 cm from the end. The thermocouples were remounted to the heat pipe using small spring type clamps. The clamps were 0.8 cm wide and 0.06 cm thick. A 13th thermocouple was used to measure the air temperature around the heat pipe.

The thermocouples were tested to determine their accuracy using a boiling water bath. From atmospheric conditions on the day of the test, the temperature of the boiling water was determined to be 93 C. The thermocouples gave readings ranging from 93.3 to 93.6 C. Therefore, the thermocouples' offset was always <0.6 C. The thermocouples were also tested in an ice bath.

A Superior Electric Co. Powerstat (Variable Transformer) was used to regulate the power to the electric heater. Two Simpson True RMS Digital Multimeters were used to monitor the current and voltage supplied by the Powerstat. The error in the power calculations was at most 1%.

A Keithley Series 500 Data Acquisition System connected to an IBM PC-XT Computer using Labtech Notebook Version 4, Laboratory Technologies Corp., software performed the data acquisition role during the experiment.

The startup studied was caused by a 23-W step increase in power at the evaporator end of the heat pipe.

Comparison of Results

The numerical results presented consist of temperature vs time graphs for the heat-pipe startup. The temperature graphed is a temperature midway along the evaporator end of the heat pipe on the outside surface.

Some general trends were noticed in the data that are not included in the figures that follow. For all numerical runs, the outside heat-pipe wall temperatures for the evaporator were essentially the same at all axial locations as were the outside condenser wall temperatures. The condenser temperatures always lagged behind the evaporator temperatures by <10°C. The water vapor's temperature, pressure, and density would vary with time (increasing as the heat pipe started) but varied very slightly axially along the heat pipe at any given time. The evaporation and condensation velocity V was essentially constant axially along the heat pipe at any given time, only changing sign between the evaporator and condenser. The water vapor's axial velocity u would increase axially along the evaporator, reach a maximum at the evaporator/condenser interface, and then decrease along the condenser. All of the different properties behaved as expected.

Acceleration Techniques

Time Warping

Figure 4 presents the results of the time warp studies. Recall that time warping is marching the wall model at a different time step than the vapor model. The model used to obtain the dashed line results in Fig. 4 marched the wall and vapor models through time using the same time step. The solution

required 46.9 CPU hours on a VAX 8600 computer. The solid line in Fig. 4 represents results where the wall was marched through time using a time step 500 times larger than the time step used for the vapor (warp 500). This solution required only 6.1 CPU minutes of computer time.

One might ask why this can be done. For the transient heat-pipe problem, the vapor transient and the wall transient can have vastly different time scales. The wall problem's time scale is related to the thermal capacitance of the heat-pipe wall, whereas the vapor problem's time scale is related to the speed of sound in the vapor. The two time scales can be different by several orders of magnitude.

The physics included in the vapor model and the solution technique are able to model rapid transients that might occur in the vapor space; however, the relatively slow heat transfer transient in the heat pipe wall prevents fast vapor transients from occurring. Time warping effectively speeds up the wall transient, which the vapor model can accurately track.

As discussed earlier, the only limitations of the warping method are the stability constraints of the wall and vapor models. The maximum time step allowed in the wall model is limited by the stability constraint of the wall model solution technique.

Implicit vs Explicit Results

Figure 5 compares results from the implicit and explicit models when modeling essentially the same problem. The warp 1 explicit results required 10 times more computer time than the implicit results.

The explicit code, with a warp of 10 (wall model using a time step 10 times the vapor time step), could perform as fast

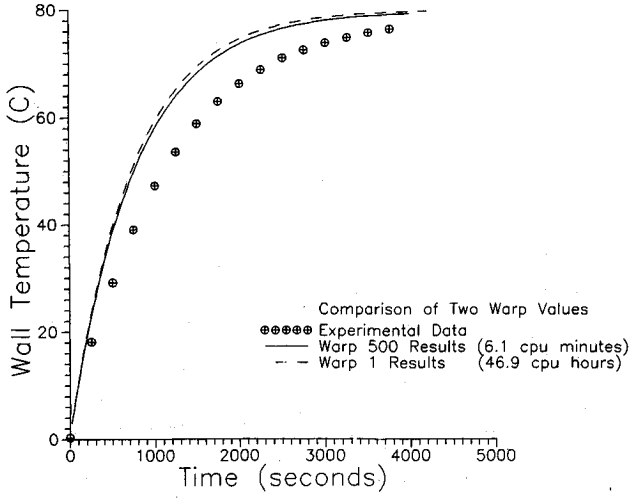

Fig. 4 Comparison of two warp values.

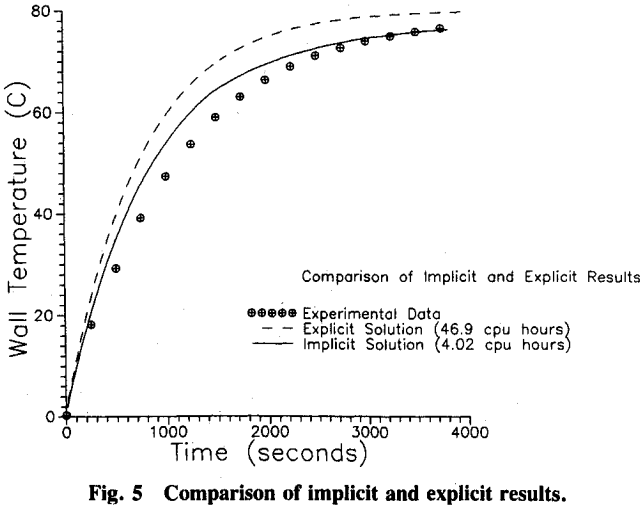

Fig. 5 Comparison of implicit and explicit results.

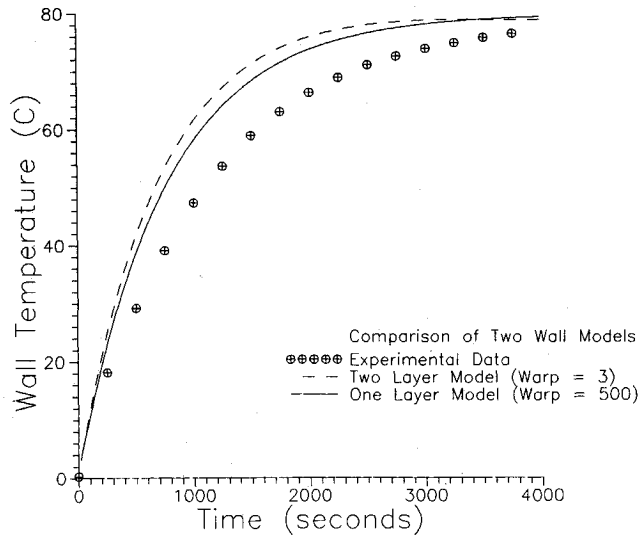

Fig. 6 Comparison of two wall models.

as the implicit model with no warp. Time warping might be able to speed up the implicit solution like it does the explicit. This is another area for more investigation.

Different Wall Model Results

Figure 6 compares the results of the one-layer model (wall assumed to consist of one homogeneous layer, discussed earlier) and the two-layer model (wall assumed to consist of an outer copper layer and an inner wick/liquid layer). Both models are shown to give comparable results.

One advantage of the one-layer model over the two-layer model was reduced computer time requirements. As discussed earlier, the maximum time step allowed by the wall model depended on the thermal diffusivity of the wall material. The smaller the thermal diffusivity, the larger the allowable time step [Eq. (19)]. For the one-layer model, a thermal diffusivity of 0.705×10^{-6} m^2/s was used corresponding to a wall made of 31.4% water (% by volume) and 68.6% copper. For the two-layer model, two values of thermal diffusivity were needed: a value of 117×10^{-6} m^2/s for the copper shell, and a value of 0.333×10^{-6} m^2/s corresponding to the wick/liquid region, which was 62.9% water and 37.1% copper. The time step used for the one-layer model was based on the one-layer thermal diffusivity. The time step for the two-layer model was based on the much larger, more limiting, thermal diffusivity of the copper wall. This resulted in a much smaller time step for the two-layer model than the one-layer model and, thus, larger computer time requirements.

Conclusions

Heat-pipe transients can be successfully modeled numerically. The amount of computer time needed to obtain a solution can be greatly reduced by using time warping (marching the vapor and wall solutions through time using different time steps). Time warping seems to have a very small effect on time accuracy for the heat-pipe model used for this work.

Another way of decreasing the computer time requirements is to use the Beam and Warming implicit solution method instead of the MacCormack explicit method (at warp 1). For the same grid and no time warping, the implicit code was about 10 times faster than the explicit code.

Two methods of modeling the wall were compared in the paper. Both gave similar results and used the same amount of computer time (at warp 1). A major advantage of the single layer wall model was that a larger amount of time warping could be used resulting in CPU time reduction from 46.9 CPU hours (either model, warp 1) to 17.9 CPU hours (two-layer model, warp-3) to 6.1 CPU minute (one-layer model, warp-500) for a typical 1-h heat-pipe transient.

Acknowledgments

Special thanks need to go to Derek Hebda, an Aeronautical Engineering student at the University of Illinois at Champaign/Urbana, who helped with this study.

References

[1]Hall, M. L., and Doster, J., "Transient Thermohydraulic Heat Pipe Modeling," Proceedings of the 4th Symposium on Space Nuclear Power Systems, Albuquerque, NM, Jan. 1987.

[2]Costello, F. A., Merrigan, M., and Read, R., "A Detailed Transient Model of a Liquid-Metal Heat Pipe," Proceedings of the 4th Symposium on Space Nuclear Power Systems, Albuquerque, NM, Jan. 1987.

[3]Ransom, V. H., and Chow, H., "ATHENA Heat Pipe Transient Model," Proceedings of the 4th Symposium on Space Nuclear Power Systems, Albuquerque, NM, Jan. 1987.

[4]Beam, J. E., "Transient Heat Pipe Analysis," AIAA Paper 85-0936, AIAA 20th Thermophysics Conference, Williamsburg, VA, 1985.

[5]Colwell, G. T., "Transient Heat Pipe Operation in the Near Critical Region," Proceedings of the Fourth International Heat Pipe Conference, London, Sept. 1981.

[6]Bowman, J., and Sweeten, R. W., "Numerical Heat-Pipe Modeling," AIAA Paper 89-1705, June 1989.

[7]Bowman, J., and Hitchcock, J., "Friction Coefficients for Flow in Pipes with Mass Injection and Extraction," *Journal of Thermophysics and Heat Transfer*, Vol. 3, No. 1, 1989, pp. 92–94.

[8]Bowman, W. J., "Transient Heat-Pipe Modeling, The Frozen Start-up Problem," AIAA Paper 90-1773, June 1990.

[9]Chi, S. W., *Heat Pipe Theory and Practice*, McGraw-Hill, New York, 1976.

[10]MacCormack, R. W., "The Effect of Viscosity in Hypervelocity Impact Cratering," AIAA Paper 69-354, 1969.

[11]Anderson, D. A., Tannehill, J. C., and Pletcher, R. H., *Computational Fluid Mechanics and Heat Transfer*, McGraw-Hill, New York, 1984, pp. 489–496.